

# PCCP

Accepted Manuscript



This is an *Accepted Manuscript*, which has been through the Royal Society of Chemistry peer review process and has been accepted for publication.

*Accepted Manuscripts* are published online shortly after acceptance, before technical editing, formatting and proof reading. Using this free service, authors can make their results available to the community, in citable form, before we publish the edited article. We will replace this *Accepted Manuscript* with the edited and formatted *Advance Article* as soon as it is available.

You can find more information about *Accepted Manuscripts* in the [Information for Authors](#).

Please note that technical editing may introduce minor changes to the text and/or graphics, which may alter content. The journal's standard [Terms & Conditions](#) and the [Ethical guidelines](#) still apply. In no event shall the Royal Society of Chemistry be held responsible for any errors or omissions in this *Accepted Manuscript* or any consequences arising from the use of any information it contains.

# Negative photoconductivity of InAs nanowire

Yuxiang Han,<sup>a</sup> Xiao Zheng,<sup>a</sup> Mengqi Fu,<sup>a</sup> Dong Pan,<sup>b</sup> Xing Li,<sup>a</sup> Yao Guo,<sup>a</sup> Jianhua Zhao,<sup>b</sup> Qing Chen<sup>a,\*</sup>

<sup>a</sup>*Key laboratory for the Physics and Chemistry of Nanodevices and Department of Electronics, Peking University, Beijing 100871, People's Republic of China*

<sup>b</sup>*State Key Laboratory of Superlattices and Microstructures, Institute of Semiconductors, Chinese Academy of Sciences, Beijing 100083, China*

\*Corresponding author: [qingchen@pku.edu.cn](mailto:qingchen@pku.edu.cn)

**Abstract:** Negative photoconductivity is observed in InAs nanowires (NWs) without surface defected layer. The negative photoconductivity is strongly depended on the wavelength and intensity of the light, and is also sensitive to the environmental atmosphere. Two kinds mechanisms are distinguished to work together. One is related to gas adsorption, which is photodesorption of water molecule and photo-assisted chemisorption of O<sub>2</sub> molecule. The other one can be attributed to the photogating effect introduced by the native oxide layer outside the NWs.

**Keywords:** InAs nanowire, negative photoconductivity, gas adsorption, photodesorption, photogating

## Introduction

III-V nanowires (NWs) have attracted great attentions as building blocks for optical and electronic applications. Among III-V materials, InAs has small electron effective mass, high carrier mobility, narrow bandgap and ease of Ohmic contact formation<sup>1,2</sup>. These distinct properties make InAs NW a promising candidate for many important applications, such as high frequency RF transistors, single-electron transistors, terahertz sources and detectors, etc. In particular, novel optoelectronic devices have been demonstrated based on InAs NWs, including broad spectrum

photodetectors ranging from ultraviolet to infrared regions, photovoltaic cells and solar cells.<sup>3-7</sup> For instance, vertical InAs NW array photovoltaic cell based on heterojunction at the interface between InAs NW and Si substrate has shown broad spectral response from visible to infrared region.<sup>6</sup> Near-infrared photodetectors with detection wavelength up to  $\sim 1.5 \mu\text{m}$  has been achieved in single-crystal InAs NW grown by molecular beam epitaxy (MBE) with an external photoresponsivity of  $5.3 \times 10^3 \text{ AW}^{-1}$ .<sup>3</sup> In all these optoelectronic applications, the conductivity of the InAs NWs increases with light exposure, the so called positive photoconductivity. Recently, negative photoconductivity has been reported in InAs NW field effect transistors (FETs).<sup>8</sup> The defected outer layer in the InAs NWs grown by chemical vapor deposition (CVD) was believed to work like a photogating layer under the light and induce the negative photoconductivity. A high photoconductive gain of approximately  $10^5$  and a fast response time of 12 ms have been reported at room temperature due to the majority-carrier-dominated photodetection mechanism. It is well known that InAs NWs are very sensitive to chemical molecules owing to their high surface-to-volume ratio, high surface electron concentration layer and rich surface states.<sup>9-12</sup> The positive photocurrent has been observed to decrease when the InAs photodetectors are exposed to the ambient atmosphere.<sup>3</sup> However, the negative photoconductivity due to the photogating layer has been reported to be free from the environmental impact.<sup>8</sup> Here, we report negative photoconductivity in single crystalline InAs NW without surface defected layer. The present negative photoconductivity is found to depend strongly on the wavelength and intensity of the light, and be sensitive to the environmental atmosphere. The mechanism of the negative photoconductivity is found to be complex.

The InAs NWs used in the present work were grown by MBE without intentionally doping.<sup>13</sup> The as-grown InAs NWs have diameter of 20 to 30 nm and are covered by a native oxide layer  $\sim 2$  nm in thickness. The NWs are characterized to have single crystalline zinc blende (ZB) or wurtzite (WZ) structure and very smooth surface through high-resolution transmission electron microscopy (HRTEM) images and their fast fourier transformations, as shown in Figure 1(a). To fabricate the InAs

NW FETs as shown schematically in Figure 1(b), the NWs were transferred onto a pre-cleaned Si/SiO<sub>2</sub> (300 nm) substrate and located by scanning electron microscopy (SEM). Source and drain (S/D) electrodes were defined by electron beam lithography (EBL) and composed of Cr/Au (25/50 nm) deposited by electron beam evaporation. The native oxide of the NWs in the contact area was etched by diluted NH<sub>4</sub>S<sub>x</sub> solution before the S/D metal deposition. Figure 1(c) shows a SEM image of a typical FET with the NW diameter being 23 nm and the channel length being 2.2 μm. Optoelectronic measurements of the InAs NW transistors were performed with a LabRAM HR800 Evolution system, a Probe Station and a Keithley 4200 semiconductor analyzer.

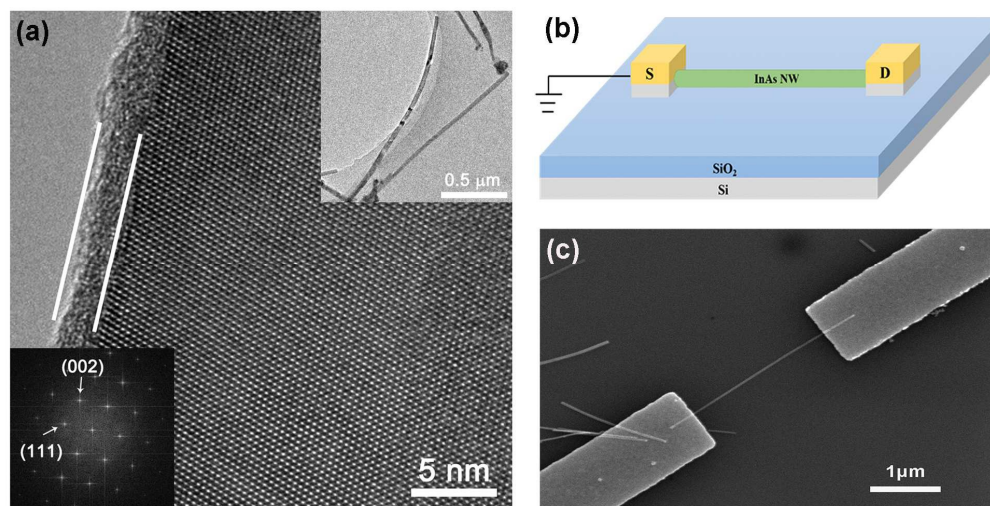


**Figure 1.** (a) HRTEM image and corresponding Fourier transformation pattern (the low-left inset) of an InAs NW with ZB structure. The up-right inset is a low magnification image. (b) Schematic diagram showing the structure of a NW FET. (c) SEM image of an InAs NW back-gate FET.

## Results and discussion

Figures 2(a) and 2(b) show the typical transfer and output curves of an InAs NW back-gate FET. The on/off ratio is about 3 orders of magnitude. The linear relationship between  $I_{ds}$  and  $V_{ds}$  indicates the contact is ohmic contact. According to our experience, such device characters indicate the devices are based on InAs NW with ZB structure.<sup>14</sup>

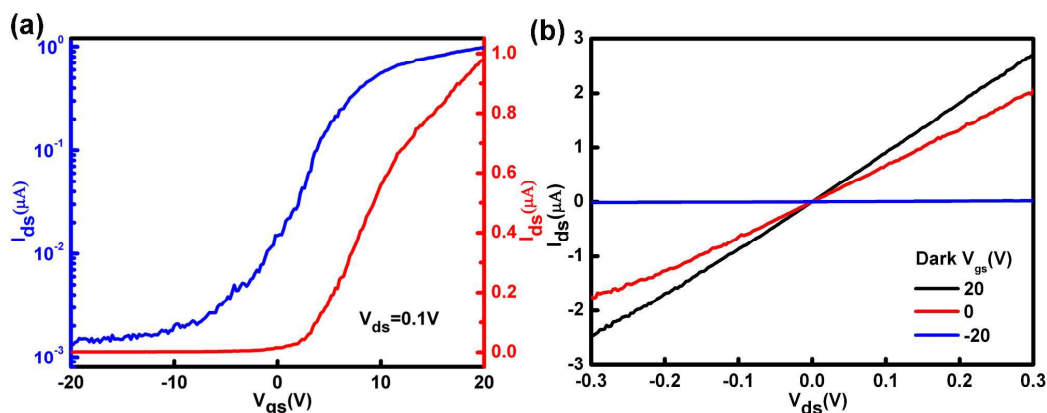


**Figure 2.** (a)  $I_{ds}$ - $V_{gs}$  and (b)  $I_{ds}$ - $V_{ds}$  curves of an InAsNW back-gate FET.

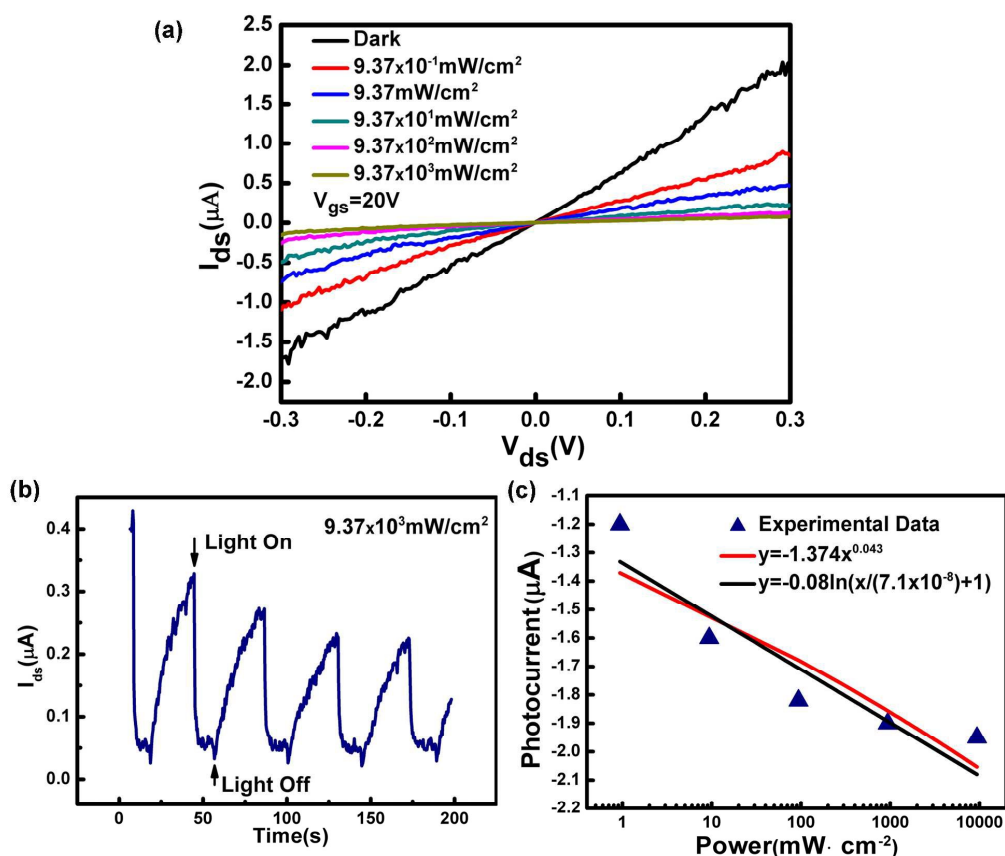


**Figure 3.** (a)  $I_{ds}$ - $V_{ds}$  curves of a single InAs NW FET in dark and under different light intensity illumination at  $V_{gs}=20V$ . (b) Time-resolved current rise and decay curve as obtained by application and removal of 633nm light illumination at  $V_{ds}=0.1V$ ,  $V_{gs}=20V$  and light intensity of  $9.37 \times 10^3 \text{ mW}\cdot\text{cm}^{-2}$ . (c) Photocurrent under  $V_{ds}=0.3V$  vs light intensity and the fitting curve.

Firstly, a 633 nm laser is used to investigate the photoelectric response properties of the InAs NWs in ambient air, as InAs NW photodetectors have been reported to have the highest photoelectric response at light wavelength around 600 nm.<sup>4</sup> In

contrast to the previously observed positive photoelectric response,<sup>3-5</sup> negative photoconductivity is observed from the output characteristics of the present InAs NW FETs at the on-state ( $V_g=20$  V), as displayed in Figure 3(a). The current decreases under light illumination and the amount of the current drop increases as the light intensity increases. The largest current drop is obtained under the highest light intensity we used, which is  $9.37 \times 10^3 \text{ mW}\cdot\text{cm}^{-2}$ . Similar to the positive photoelectric response, we denote the photocurrent  $I_{\text{ph}}$  being the current change with the light illumination,  $I_{\text{ph}}=I_{\text{light}}-I_{\text{dark}}$ , where  $I_{\text{light}}$  and  $I_{\text{dark}}$  are the current with and without light illumination. The largest photocurrent we observed at  $V_{\text{ds}}=0.3$  V and  $V_{\text{gs}}=20$  V is  $-1.97 \mu\text{A}$ , which value is about 96% of  $I_{\text{dark}}$  at the same measuring condition.

Figure 3(b) illustrates the time-resolved current change obtained by introducing and removal the 633 nm laser. It shows when the light was turned on at 12 s, the current decreased dramatically to a low value in less than 0.25 s (which is the minimum interval between two points in our measurement setting). Keeping the light on for about 10 s, the current remained roughly the same at about  $0.05 \mu\text{A}$ . When the light was moved away from the FET, the current first decreased a little, and then increased continuously to saturation. Negative photoelectric response is repeatable in light switching cycles. The same phenomena is also observed for different light intensity (as shown in Figure S1 in the Supporting Information). The negative photoconductivity in the InAs NW device is enhanced and tend to saturate at higher light intensity.

Although the phonon energy of the 633 nm light ( $E=hc/\lambda$ , 1.96 eV) is much higher than the InAs NW's bandgap (about 0.35 eV), and should be able to generate electron-hole pairs and introduce positive photoelectric response in the InAs NW, we only observe a small positive photoelectric response from the little current decrease when the light is just moved away from the FET, and such phenomena does not show when the light intensity is smaller than  $9.37 \times 10^3 \text{ mW}\cdot\text{cm}^{-2}$  (as shown in Figure S1 in the Supporting Information). The main photoelectric response of the present InAs NW FETs is the repeatable negative photoconductivity, which is the opposite to most of the previous reports.

Negative photoconductivity has been reported in CVD grown InAs NWs previously, where the InAs NWs were covered by defected outer layer.<sup>8</sup> However, the present InAs NWs are grown by MBE and have smooth surface and perfect crystalline structure. Therefore, the mechanism of the present negative photoconductivity cannot be due to the photogating effect of a defected outer layer. It has been found that in most of the cases, the photocurrent and the light intensity follow a power law relationship  $I_{ph}=C_1 \times P^{C_2}$ , where  $C_1$  is a constant corresponding to a certain wavelength and  $C_2$  determines the response of photocurrent to light intensity.<sup>15-17</sup> Even the negative photocurrent reported in the InAs NW with defected outer layer follows the power law. However, the present negative photocurrent cannot be fitted very well with a single power law, as shown in Figure 3(c). On the other hand, it has been reported that a negative photoresponse can be attributed to trapping of photogenerated carriers in the buffer layer, causing a change in the potential profile and consequent reduction in the number of carriers in the 2-DEG channel. For this mechanism, the photoresponse is a logarithmic function of the optical power, as  $I_{ph}=I_{ph0} \ln (P/P_0+1)$ , where  $I_{ph}$  is the photoresponse,  $P$  is the optical power and  $I_{ph0}$  and  $P_0$  are parameters of curve fitting.<sup>18</sup> However, the present experimental data cannot be fitted very well with this logarithmic function either, as shown in Figure 3(c). Therefore, the present negative photoresponse should have a complex photoelectric response mechanism.

The above measurements are operated in ambient air and may be affected by gases in the environment. Gas molecule adsorption and photodesorption have been proved to play an important role in photoelectric property and can lead to negative photoconductivity in some nanomaterials. For instance, in the cases of carbon nanotubes (CNTs) and single layer graphene, UV light can effectively desorb gas molecules like O<sub>2</sub>, H<sub>2</sub>O, NH<sub>3</sub> and NO<sub>2</sub> and cause negative photoelectrical response,<sup>19</sup> and such molecule photodesorption process can be utilized to clean nanotubes and enable rapid reversibility of nanotube chemical sensors.<sup>21,22</sup> Also, photodesorption of water molecules has been found in other nanomaterials, such as ZnO nanobelts<sup>20</sup> and CeO<sub>2</sub> nanowire,<sup>23</sup> and the photoresponse is dependent on relative humidity and can be

used to fabricate photoelectric humidity sensor to detect water vapor with low concentration. Due to the large surface-to-volume ratio, the presence of surface states and the existence of an electron surface accumulation layer, InAs NWs are easy to adsorb gas molecules and have their electric properties changed.<sup>10-12</sup> Previous study has proved that PMMA can work as a passivation layer to suppress the effects of atmospheric molecules.<sup>25</sup> To isolate the InAs NW FETs from air, a layer of PMMA (950K A4, about 300 nm thick) was spin coated onto the chip and the sample was baked on a hotplate at 150 °C for 5 minutes. The current response curve measured from an InAs NW FET coated by PMMA is shown in Figure 4(a). The inset in Figure 4(a) shows the result measured from the same FET without PMMA coating for comparison. The laser with 405 nm wavelength is employed here because the photon energy is higher and the UV light can desorb gas molecules efficiently.<sup>21-24</sup>

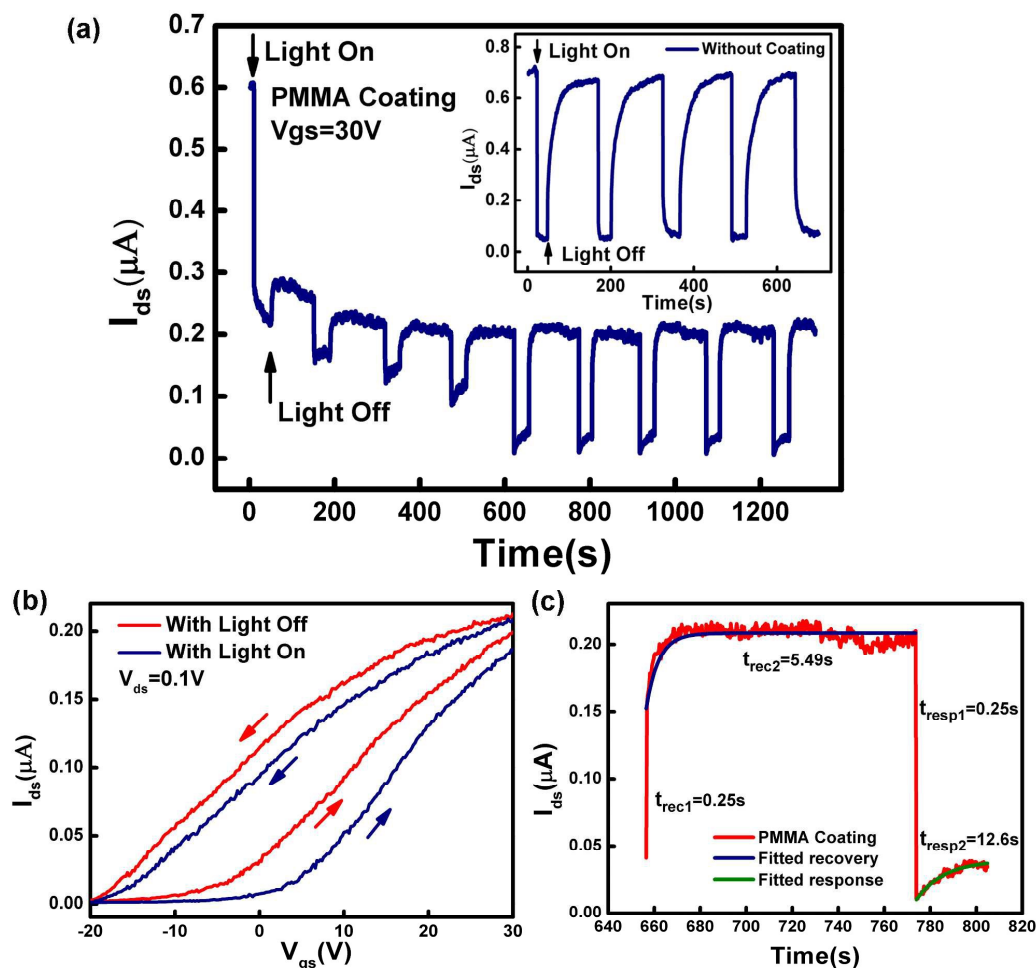


**Figure 4.** (a) Time-resolved current rise and decay curve as obtained by application and removal



of 405 nm light illumination on a PMMA-coated InAs NW FET. Inset is the current-time curve of the InAs NW device without PMMA coating. (b)  $I_{ds}$ - $V_{gs}$  curves without/with light illumination obtained at the stable state after four light switching cycles in (a), the arrows point the sweeping direction. (c) fitting curves of one light switching cycle at stable state in (a).

As shown in the inset of Figure 4(a), in the air, the current response of the uncoated InAs FET to the 405 nm laser is even more repeatable than to the 633 nm laser. However, the PMMA coated InAs FET does not have a repeatable current response at the beginning, as is displayed in Figure 4(a). When the FET was firstly illuminated by the 405 nm laser at an intensity of  $9.93 \times 10^3 \text{ mW}\cdot\text{cm}^{-2}$ ,  $I_{ds}$  at  $V_{gs}=30 \text{ V}$  and  $V_{ds}=0.1 \text{ V}$  decreases from the original  $0.6 \mu\text{A}$  to about  $0.2 \mu\text{A}$ . When the light was moved away from the PMMA-coated InAs NW FET, only a small portion of the photocurrent recovered. When the light exposed to the device again, the current decrease to a level lower than the first current decrease. After four light on/off cycles, the transistor reached a stable state: the current change with/without light illumination can repeat steadily. It should be noted that the minimum  $I_{light}$  is only  $0.9 \text{ nA}$  (at the stable state), which is only about  $0.15\%$  of the original  $I_{dark}$  and is much smaller than the  $I_{light}$  in the ambient air without PMMA coating.

The above experiment results indicate that there are two mechanisms working together on the present negative photoconductivity. One mechanism is related to the gases in the ambient air, while the other mechanism cannot be eliminated by the PMMA coating, so that should come from the InAs NW FET itself. The  $I_{ds}$ - $V_{gs}$  curves with/without light illumination were measured at the stable state as shown in Figure 4(b). Upon light illumination, the threshold voltage shifted positively from  $-3.98 \text{ V}$  to  $3.93 \text{ V}$ , but the transconductance and the on-state current are almost unchanged. The positive shift of the transfer curve means electron concentration is reduced in the conducting channel. So that at the same gate voltage,  $I_{light}$  is lower than  $I_{dark}$  and exhibits a negative photoconductivity. This phenomenon can be ascribed to a photogating effect.<sup>26</sup> The current response also correspond to a fast and a slow processes (shown in Figure 4(c)) with the time constants at the same level as that reported for the negative photocurrent caused by the photogating of the defected outer

layer,<sup>8</sup> supporting a photogating mechanism. However, the present InAs NWs have a smooth surface and perfect crystalline structure. We therefore propose the photogating effect is probably caused by the native oxide layer outside the NW.

It is well known that InAs exposed to the air is covered by a native oxide layer. According to previous XPS study,<sup>27</sup> the native oxide layer covering InAs NW is composed of  $\text{AsO}_x$  and/or  $\text{In}_2\text{O}_3$ , it is soft, hygroscopic, compositionally and structurally inhomogeneous with a large number of surface defect states which induce the surface Fermi level pinning of InAs NW in conduction band and can trap photogenerated electrons, giving rise to photogating effect. The photoelectrical response process could be described as followed. Before light illumination, the free electrons in the InAs NW flow under the action of the electric field to form the dark current. Upon light illumination, the photogenerated electrons from the core are excited into the native oxide layer and trapped by the surface trapping centers, leaving unpaired holes to recombine with the free electrons. Meanwhile, the trapped electrons in the native oxide layer generate a built-in electric field to deplete free electrons in the core further through capacitive coupling. The synergistic effect of these two processes results in a large decrease of the current under the light illumination, so that a negative photoconductivity is observed.

The unstable current response in the first several light on/off cycles in the PMMA-coated FET (shown in the main body of Figure 4a) can be understood through the gas-related mechanism. Before PMMA coating, the NW has been exposed to the air and has already adsorbed some gases on its surface. The PMMA coating itself cannot remove these gas adsorptions. With the light illumination, the existed adsorbed gases on the PMMA-coated InAs NW desorb and the current drops. When the light is moved away, due to the PMMA coating layer, the gases cannot reach the surface of the InAs NW and be adsorbed again, so that this part of current cannot recover. When the PMMA-coated InAs NW FET is illuminated by the light for the first time, not all the adsorbed gases can desorb, so that  $I_{\text{off}}$  is not the lowest. But when the light exposes to the InAs NW again, the resident adsorb gases desorb further,  $I_{\text{off}}$  decreases further. After several light on/off cycles, all the desorbable gases desorb and  $I_{\text{off}}$

decreases to the minimum value.

Now we consider which gas in the air introduces the above photocurrent. The major components in the air are  $N_2$ ,  $O_2$  and  $H_2O$ . Previous work on InAs NW gas sensor have reported that  $N_2$  molecules have little effect on the NW conductance and their effect can be neglected.<sup>10</sup> Water molecule adsorbed on InAs NW can increase the NW conductance.<sup>10,12</sup> However, the impact from  $O_2$  molecule on the InAs NW is seldom studied. To understand the effect of different gases, we here measure the  $I_{ds}$ - $V_{gs}$  curves of uncoated FETs with/without light illumination in the air, water and  $O_2$  atmosphere, and compare them with that in the vacuum measured just before the measurements in the gases.

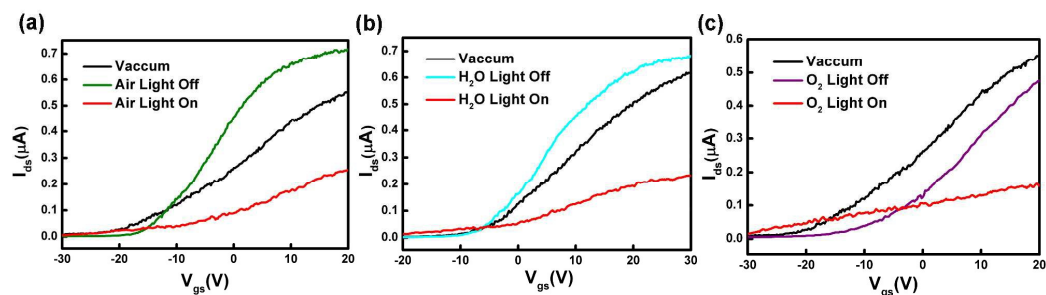


**Figure 5.**  $I_{ds}$ - $V_{gs}$  curves of an InAs NW FET at  $V_{ds}=0.1V$  in different atmosphere: (a) in the air, (b) in the 2338 Pa water atmosphere (the saturated water vapor pressure at room temperature). (c) in the 1atm  $O_2$  atmosphere. The curves in the vacuum were measured without light illumination just before introducing gases.

As shown in Figure 5(a), without light illumination, the on-state current of the uncoated FET is larger in the air than in the vacuum. When exposed to the light, the on-state current in the air drops to a value even smaller than the current in the vacuum without light exposure. The on-state current of the FET in water vapor changes in a similar way as that in the air. As shown in Figure 5(b), without light illumination, compared with the transfer curve in the vacuum, the on-state current  $I_{ds}$  increases, e.g. the current at 30V gate voltage increases from 0.61  $\mu A$  to 0.68  $\mu A$ . However, the threshold voltage of the InAs NW FET in water atmosphere only shift positively a

little from -6.12 V (vacuum) to -5.46 V (water). Generally, water molecules adsorbed on a semiconductor behave as electron donor and increase the electron concentration in the material. This is confirmed in the present experiment by the increase of the on-state current. Additionally, the transconductance and the field effect mobility of the InAs NW FET are enhanced in the water atmosphere. The transconductance is obtained from the transfer curve using the equation:

$$g_m = \left. \frac{\partial I_{ds}}{\partial V_{gs}} \right|_{V_{ds}}$$

And the field effect mobility is calculated by:

$$\mu_n = \frac{L^2 \cdot g_m}{C_g \cdot V_{ds}}$$

Where  $L$  is the channel length,  $C_g$  is the gate capacitance. The maximum transconductance is 20 nS in the vacuum and 38 nS in the water atmosphere. The field effect mobility is 412 cm<sup>2</sup>/V·s in the vacuum and 783 cm<sup>2</sup>/V·s in water atmosphere. The mobility increase in the water atmosphere could be possibly due to the mechanism that the adsorption of water molecule might reduce the traps at the surface of the InAs NW or in the native oxide layer so that reduce carrier scattering.

When the device in the water atmosphere is exposed to the light with 405 nm wavelength and 9.93 x10<sup>3</sup> mW·cm<sup>-2</sup> light intensity, negative photoconductivity is observed at the on-state, the threshold voltage shifts to about -5.86V, and a weak positive photocurrent can be observed at the off-state. These changes can be explained by the energy band diagram shown in Figures 6(a) and Figure 6(b). Before light illumination, the Fermi level of the InAs NW near the surface is pinned near the conductance band, and under a gate voltage larger than the threshold voltage the InAs NW is at the on-state. When InAs NW is placed in the water atmosphere, water molecules can chemisorb on the surface of InAs NW and donate electron to the NW so that cause downward of the conduction band. Therefore, the current increase after water molecule adsorption. Under the illumination of a light with its photon energy higher than the bandgap of InAs NW, photogenerated electron-hole pairs are generated in the NW. The electron-hole pairs are separated and the electrons migrate

to the surface due to the presence of the built-in electric field near the surface. The photogenerated electron can recombine with the positive water ion and desorb water molecule from the InAs NW surface, and the photogenerated holes can recombine with the carrier electrons and reduce the carrier concentration in the channel, so that a negative photoconductivity can be observed.

However, electrical properties of InAs NW FET in the O<sub>2</sub> atmosphere is different from that in the water atmosphere. Compared with that in the vacuum, the threshold voltage of InAs NW FET in the O<sub>2</sub> atmosphere shift positively from -14.64 V (in the vacuum) to -6.93 V (in O<sub>2</sub>), but the transconductance in these two atmosphere is almost unchanged, as shown in Figure 5(c). The maximum transconductance of the FET is 25 nS in the vacuum and 26 nS in O<sub>2</sub>, hence there is little difference in the field effect mobility between these two situations. However, the on-state current in O<sub>2</sub> atmosphere is nearly the same as that in the vacuum at the same  $V_g - V_{th}$ , where  $V_g$  is the gate voltage and  $V_{th}$  is the threshold voltage. It is worth mentioned that the transfer curve in the vacuum is measured every time before a gas is introduced, as the experiments on the water and oxygen effects were performed in different days, the transfer curves in the vacuum corresponding to these two atmospheres are different.

O<sub>2</sub> molecule is commonly considered as an electron acceptor and O<sub>2</sub> molecule adsorb on the NW surface can capture free electrons from the NW and reduce the electron density in the channel.<sup>17</sup> Light exposure can cause discharge of the adsorbed O<sub>2</sub> ions through surface electron-hole recombination and introduce positive photoconductivity.<sup>17</sup> However, in the present experiments, O<sub>2</sub> adsorption in the dark only causes the transfer curve shift positively but does not change the on-state current. Therefore, the adsorption of O<sub>2</sub> in the dark acts like a negative gate applied to the InAs NW FET, so that a more positive gate voltage is needed to switch on the transistor. The electron concentration in the channel does not change by the adsorption of O<sub>2</sub>, probably due to the native oxide layer covering the InAs NW. So that, the adsorption the O<sub>2</sub> in the dark is probably a physical adsorption on the surface of oxide-covered InAs NW, as shown in Figure 6(c).

Under light exposure in O<sub>2</sub> atmosphere, the on-state current of the FET decreases

greatly, the off-state current increases a little and the gate control ability becomes weak. The small positive photocurrent at the off-state is in consistence with the positive photoconductivity reported previously and can be understood by the light-induced electron-hole pairs which increase the carrier concentration. The negative photocurrent at the on-state cannot be explained by the light-induced discharge of the adsorbed  $O_2$  ions reported previously.<sup>17</sup> So far, we cannot fully explain the phenomena yet, but propose a possible mechanism here. When the light illuminates the NW, electron-hole pairs are generated. The photogenerated electrons have higher energy than the electrons at the edge of the conductive band and could tunnel through the barrier of the native oxide outside the InAs NW and be captured by the adsorbed  $O_2$  molecules to form  $O_2^-$ , which means changing the physical adsorption to the chemisorption of  $O_2$  molecules. The photogenerated holes could combine with the carrier electrons and reduce the carrier concentration in the channel and cause the negative photoconductivity. Further work is needed to fully understand the mechanism of the negative photoconductivity in  $O_2$  atmosphere.

The negative photoconductivity in ambient air under light illumination results from the combined effects of  $H_2O$  and  $O_2$ . As shown in Figure 5(a), compared with the transfer curve in the vacuum, the curve measured in the air shows a positive shift of the threshold voltage from -15.99 V (in the vacuum) to -13.12 V and the on-state current is increased from 0.55  $\mu A$  (in the vacuum) to 0.72  $\mu A$ . The positive shift of the threshold voltage can be explained as the floating gate effect caused by the physical adsorbed  $O_2$  molecule and the increase of the on-state current is caused by the water molecule adsorption. As the influence of the water molecule is dominant, the current increases rather than decreases at the on-state in the dark. Under light illumination, the negative photoconductivity at the on-state is observed because of the photodesorption of water molecule and the photo-assisted oxygen chemisorption processes.

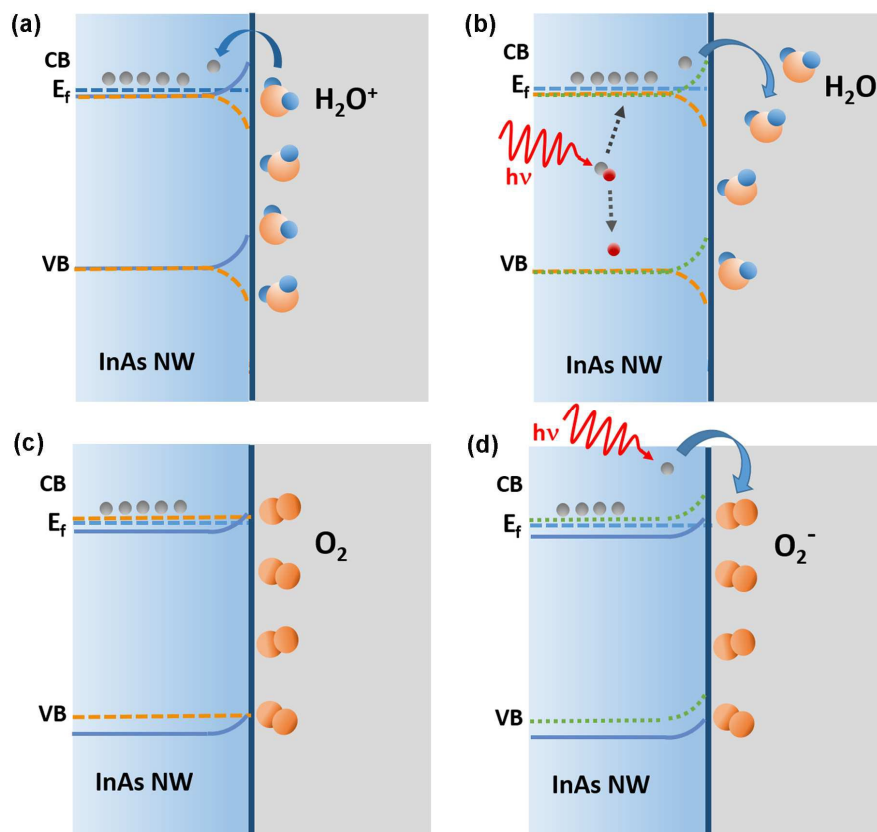


**Figure 6.** Theoretical models of the interaction process of InAs NW with water molecules and oxygen molecules in dark (a) (c) and under light illumination (b) (d). VB and CB represent the valence band and conduction band, respectively. The blue solid lines represent the position of the energy level before gas adsorption, the orange dashed lines represent the energy level after gas adsorption and the green dashed lines indicate the energy level after light exposure.

Response time is a key factor that can reflect the mechanism of the light response. The on-state current is measured at  $V_{ds}=0.1$  V and  $V_g=30$  V with the light switches on and off in the air, water and oxygen atmosphere, as shown in Figures 7(a), 7(b) and 7(c). Negative photoconductivity can be rapidly stimulated by switching on the light (405 nm,  $9.93 \times 10^3$  mW $\cdot$ cm $^{-2}$ ), and the current can recover to its origin value after a relatively long time exposure in the gas atmosphere without light illumination. These light switching cycles have a good stability. Within the four cycles we measured every time, the response speed and the maximum/minimum current of each cycle remain unchanged. As shown clearly in Figures 7(d), 7(e) and 7(f), there are four processes in

each switching cycle: fast response process, slow response process, fast recovery process and slow recovery process. The response process and recovery process can be well fitted with two first-order kinetic processes:

$$I = I_0[1 - A_1 \exp(-t / \tau_{resp1}) - A_2 \exp(-t / \tau_{resp2})] \quad \text{and}$$

$I = I_0[1 - B_1 \exp(-t / \tau_{rec1}) - B_2 \exp(-t / \tau_{rec2})]$ , where  $I_0$  is the dark current,  $\tau_{resp1}$ ,  $\tau_{resp2}$ ,  $\tau_{rec1}$ ,  $\tau_{rec2}$  are the time constants related to the response and recovery process. The time constants are obtained from fitting the experimental switching cycle curves. Taking water atmosphere for example, the fast response time is 0.21 s, which is smaller than our sampling value interval and the actual fast response time should be shorter than 0.21 s. This first-order term meets well with the photodesorption process observed in single layer graphene and carbon nanotube.<sup>19,28,29</sup> The time constant of the slow response process is  $\tau_{resp2}=11.47$  s,  $\tau_{resp2} \gg \tau_{resp1}$  and might be attributed to zero-order kinetic term as thermal desorption process.<sup>30</sup> Usually, without light exposure, it takes tens of minutes for InAs NW to desorb water molecule and it cannot fully return to the origin state only by pumping to vacuum.<sup>10,12</sup> Our results provide a new way to fast desorb water molecule from InAs NW by light exposure and can make the gas sensors work more efficiently. Correspondingly, the fast recovery process with time constant of  $\tau_{rec1}=0.37$  s corresponding to the fast re-adsorption process by removal of light. The slow recovery process with time constant of  $\tau_{rec2}=22.65$  s corresponding to the slow re-adsorption process by reduction of temperature. This time constant is roughly the same as the time when the current of an on-state InAs NW FET increases to 90% of the highest current after re-exposed to H<sub>2</sub>O from a vacuum observed in our previous report,<sup>12</sup> supporting the slow recovery process is a re-adsorption process.

Unlike the case in water atmosphere, the time constant we extracted from oxygen atmosphere is  $\tau_{resp1}=0.18$  s,  $\tau_{resp2}=10.94$  s,  $\tau_{rec1}=1.47$  s,  $\tau_{rec2}=163.69$  s. The time constants of fast recovery process and slow recovery process are much longer than that in the water atmosphere, which means the photo-assisted chemisorbed O<sub>2</sub> molecule is hard to lost electron owing to the strong oxidizability of oxygen molecule and the electron concentration in the InAs NW channel is hard to recover. The time



constant extracted from the light switching cycle in the air is very close to the value extracted in water atmosphere with  $\tau_{\text{resp1}}=0.18$  s,  $\tau_{\text{resp2}}=8.59$  s,  $\tau_{\text{rec1}}=0.58$  s,  $\tau_{\text{rec2}}=18.50$  s, this is because the influence from water molecule adsorption and photodesorption is dominant at the on-state in air, as can be seen in Figure 5.

We also measure the light switching behavior and extract the time constant under a low pressure at  $1.3 \times 10^{-3}$  Pa, as shown in Figure S2. There is still a negative photoconductivity with the response time lies between that in the water atmosphere and that in the  $\text{O}_2$  atmosphere. This is because the above pressure is not low enough and there is still about  $10^{17}/\text{m}^3$  gas molecules in such vacuum condition, and also some adsorbed molecules can hardly desorb only by pump to vacuum. These molecules (should contain water molecules) account for the negative photoconductivity in this condition. As the density of the gas molecules is lower at this low pressure, the recovery time is longer than that in the water atmosphere.

It is noticed that in the device coated by PMMA the time constant for the recovery process ( $\tau_{\text{rec1}}=0.25$ s,  $\tau_{\text{rec2}}=5.49$ s, as shown in Figure 4(c)) is much shorter than the uncoated devices in all the atmosphere, indicating a different photoresponse mechanism. The time constant for the recovery process of the PMMA-coated devices is about the same order as that in the defected InAs NW, supporting a mechanism of photogating near the InAs NW. The present photogating is probably due to the native oxide layer.

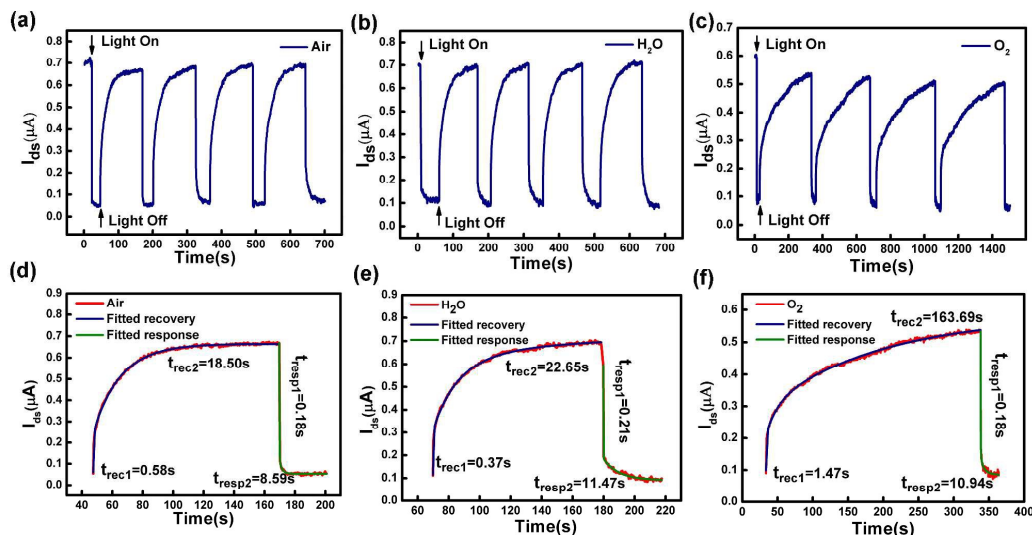


**Figure 7.** Photoelectrical response properties of InAs NW under 405 nm,  $9.37 \times 10^3 \text{ mW} \cdot \text{cm}^{-2}$  light illumination at  $V_{ds}=0.1 \text{ V}$ ,  $V_{gs}=30 \text{ V}$  in different atmosphere: (a) in the air, (b) in the water atmosphere, (c) in the  $\text{O}_2$  atmosphere and (d) (e) (f) show the fitting curves.

Previous research have shown that UV light can desorb gas molecules effectively.<sup>21-24</sup> Also, photogating effect has higher response under short wavelength light.<sup>8</sup> As for photo-assisted chemisorption of  $\text{O}_2$  molecule, shorter wavelength light with higher phonon energy can increase the tunneling probability of electron being accepted by the physical-absorbed  $\text{O}_2$  molecule. Based on all these consideration, we propose that shorter wavelength light can induce more significant negative photoconductivity. To testify this proposal, we expose the same InAs NW FET shown in Figures 2(a) and 2(b) by the light with different wavelength in ambient air. Figures 8(a), 8(b) and 8(c) are the transfer curves acquired under the light illumination with different light intensity with the wavelength of 488 nm, 633 nm and 785 nm.

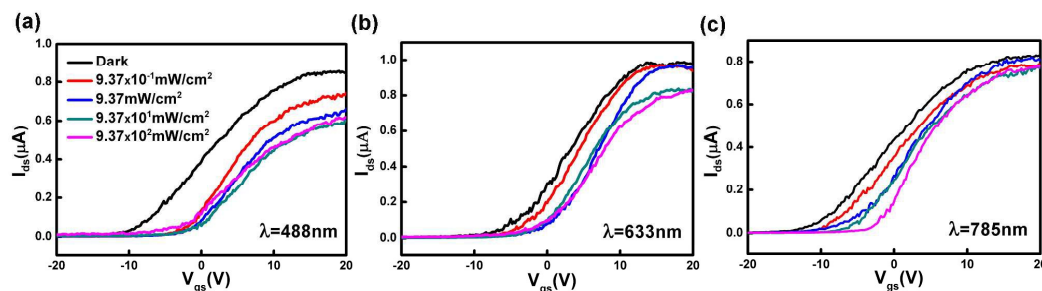


**Figure 8.** Gate-voltage dependence of InAs NW channel current under different wavelength light irradiation: (a)  $\lambda=633 \text{ nm}$ , (b)  $\lambda=488 \text{ nm}$ , (c)  $\lambda=785 \text{ nm}$ , the gate voltage sweep from 20 V to -20 V.

The curves were measured under different light intensities as shown in (a).

Negative photoconductivity is observed at the on-state under illumination of all the three wavelength lights. As shown in Figures 8(a), 8(b) and 8(c), in all the three cases, the threshold voltage shifts to right under light illumination due to the electron depletion in the channel. The current  $I_{ds}$  at the on-state decreases continuously with the light intensity increasing from  $9.37 \times 10^{-1} \text{ mW}\cdot\text{cm}^{-2}$  to  $9.37 \times 10^2 \text{ mW}\cdot\text{cm}^{-2}$ . The maximum current decrease at  $V_{gs}=30 \text{ V}$  is  $0.25 \mu\text{A}$  for the 488 nm laser and  $0.16 \mu\text{A}$  for the 633 nm wavelength light, but only  $0.06 \mu\text{A}$  for the 785 nm laser, which means the on-state current decreases more under 488 nm laser than under 785 nm laser. According to our experiment, short wavelength light can cause stronger negative photoconductivity, this is because short wavelength light with high-energy photons can desorb water molecules more effectively and offer more energy to  $\text{O}_2$  molecules to get chemisorbed. Also, high-energy photons can excite the photogenerated electrons into the native oxide layer more efficiently, leading to a more powerful photogating effect. These results support our proposal that InAs NW FET has larger negative photoresponse to the light with shorter wavelength.

Positive photoconductivity has been reported previously in InAs NWs by several groups.<sup>3-7</sup> Photogenerated electron-hole pairs in the InAs NW can be separated by the electric field in the NW or Schottky barrier in the InAs NW/graphene heterojunction, increase the carrier density and cause positive photocurrent. Such mechanism should be stronger in thicker NW due to the larger body of the NW core. While the negative photoconductivity we report presently is due to joint effects of the surface gas adsorption and the photogating effect of the native oxide layer, both of which are surface effects. We notice that the thinnest InAs NW reported previously to have positive photoconductivity is 40 nm in diameter until now.<sup>3,4</sup> While, the NWs in our present experiments are around 23 nm in diameter, which is much thinner than in the previous reports. The high surface-to-volume ratio of the present thin NWs makes the surface effect being dominated, so that we can observe the negative photoconductivity.

In fact, we also observe a positive photoconductivity at the fully off state under intensive light, as shown in Figure 8(a) and Figure S3. Although the value of the present positive photocurrent (several tens of nA) is much smaller than the value of the negative photocurrent (several hundreds of nA), it is larger than the value of the positive photocurrent of individual InAs NW in the previous report (which is a couple of nA or even in pA range)<sup>3,4</sup>. We observe that the InAs NW FETs tend to show negative photoconductivity at the on-state or in the subthreshold region, but show a small positive photoconductivity at the fully off state when the light intensity is high. We notice that the devices in the previous reports were at the fully off state at  $V_g=0$  V,<sup>3,4</sup> that could be another reason that negative photoconductivity has not been observed previously in the NW with smooth surface.

## Conclusions

In summary, negative photoconductivity is observed in MBE-grown single crystalline InAs NW with smooth surface in the air, H<sub>2</sub>O and O<sub>2</sub> atmosphere, and at a low pressure. Higher intensity light illumination leads to larger negative photocurrent response, but the relationship between the photocurrent and the light intensity cannot be fitted well with previously reported simple models, indicating a complex photoelectric response process. Through study the devices in different atmosphere and the devices coated by PMMA, two mechanisms are distinguished to work together for the present photoelectric response. One mechanism is caused by the photogating effect of the native oxide layer covering the NW. Such photoresponse remains in the PMMA coated samples and has fast response and recover processes. The other photoelectric response mechanism is related to the gas adsorption, which is related to the photodesorption of water molecule and photo-assisted chemisorption of O<sub>2</sub> molecule. The response time is fast in ambient air, water and O<sub>2</sub> atmosphere, but the recovery time is relatively long in O<sub>2</sub> atmosphere and the response time in ambient air is mainly influenced by water molecule. The negative photoconductivity also depends on the wavelength of the light, shorter wavelength light with higher-energy photon

causes stronger negative photoconductivity. Interestingly, the InAs NW FETs tend to show negative photoconductivity at the on-state or in the subthreshold region, but show a small positive photoconductivity at the fully off state when the light intensity is high. We believe that the high surface-to-volume ratio of the present thin NWs makes the surface effect being dominated, so that the negative photoconductivity is obvious.

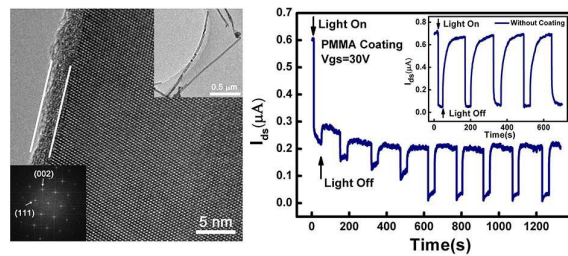
## Acknowledgments

The authors thank Dr. S. Gao for his assistance with AFM measurements. This work was supported by the MOST (Nos. 2012CB932702 and 2012CB932701) and NSF of China (Nos. 11374022, 61321001 and 11528407).

## References

1. S. A. Dayeh, D. P. R. Aplin, X. T. Zhou, P. K. L. Yu, E. T. Yu and D. L. Wang, *Small*, 2007, **3**, 326-332.
2. C. A. Mead and W. G. Spitzer, *Phys. Rev. Lett.*, 1963, **10**, 471.
3. J. S. Miao, W. D. Hu, N. Guo, Z. Y. Lu, X. M. Zou, L. Liao, S. X. Shi, P. P. Chen, Z. Y. Fan, J. C. Ho, T. X. Li, X. S. Chen and W. Lu, *ACS Nano.*, 2014, **8**, 3628-3635.
4. Z. Liu, T. Luo, B. Liang, G. Chen, G. Yu, X. M. Xie, D. Chen and G. Z. Shen, *Nano Res.*, 2013, **6**, 775-783.
5. J. S. Miao, Hu, W. D. Hu, N. Guo, Z. Y. Lu, X. Q. Liu, L. Liao, P. P. Chen, T. Jiang, S. W. Wu, J. C. Ho, L. Wang, X. S. Chen and W. Lu, *Small*, 2015, **11**, 936-942.
6. W. Wei, X. Y. Bao, C. Soci, Y. Ding, Z. L. Wang and D. L. Wang, *Nano Lett.*, 2009, **9**, 2926-2934.
7. J. C. Shin, K. H. Kim, K. J. Yu, H. F. Hu, L. J. Yin, C. Z. Ning, J. A. Rogers, J. M. Zuo and X. L. Li, *Nano Lett.*, 2011, **11**, 4831-4838.
8. N. Guo, W. D. Hu, L. Liao, S. P. Yip, J. C. Ho, J. S. Miao, Z. Zhang, J. Zou, T. Jiang, S. W. Wu, X. S. Chen and W. Lu, *Adv. Mater.*, 2014, **26**, 8203-8209.
9. M. Noguchi, K. Hirakawa and T. Ikoma, *Phys. Rev. Lett.*, 1991, **66**, 2243-2246.
10. J. Du, D. Liang, H. Tang and X. P. A. Gao, *Nano Lett.*, 2009, **9**, 4348-4351.
11. P. Offermans, M. Crego-Calama and S. H. Brongersma, *Nano Lett.*, 2010, **10**, 2412-2415.
12. X. T. Zhang, M. Q. Fu, X. Li, T. W. Shi, Z. Y. Ning, X. Y. Wang, T. Yang and Q.

- Chen, *Sens. Actuators, B.*, 2015, **209**: 456-461.
13. D. Pan, M. Q. Fu, X. Z. Yu, X. L. Wang, L. J. Zhu, S. H. Nie, S. L. Wang, Q. Chen, P. Xiong, S. V. Molnár and J. H. Zhao, *Nano Lett.*, 2014, **14**, 1214-1220.
  14. M. Q. Fu, et al. to be submitted.
  15. Y. Jiang, W. J. Zhang, J. S. Jie, X. M. Meng,; X. Fan and S. T. Li, *Adv. Funct. Mater.*, 2007, **17**, 1795-1800.
  16. P. C. Wu, Y. Dai, Y. Ye, Y. Yin and L. Dai, *J. Mater. Chem.*, 2011, **21**, 2563-2567.
  17. H. Kind, H. Q. Yan, B. Messer, M. Law and P. D. Yang, *Adv. Mater.*, 2002, **14**, 158.
  18. M. Romero and P. R. Herczfeld, *IEEE Trans. Microwave Theory Tech.*, 1995, **43**, 511-517.
  19. R. J. Chen, N. R. Franklin, J. Kong, J. Cao, T. W. Tomblor, Y. G. Zhang and H. J. Dai, *Appl. Phys. Lett.*, 2001, **79**, 2258-2260.
  20. L. Peng, J. L. Zhai, D. J. Wang, P. Wang, Y. Zhang, S. Pang and T. F. Xie, *Chem. Phys. Lett.*, 2008, **456**, 231-235.
  21. G. G. Chen, T. M. Paronyan, E. M. Pigos and A. R. Harutyunyan, *Sci. Rep.*, 2012, **2**.
  22. G. G. Chen, T. M. Paronyan and A. R. Harutyunyan, *Appl. Phys. Lett.*, 2012, **101**, 053119-053119-4.
  23. X. Q. Fu, C. Wang, P. Feng and T. H. Wang, *Appl. Phys. Lett.*, 2007, **91**, 073104-073104-3.
  24. C. Soci, A. Zhang, B. Xiang, S. A. Dayeh, D. P. R. Aplin, J. Park, X. Y. Bao, Y. H. Lo and D. Wang, *Nano Lett.*, 2007, **7**, 1003-1009.
  25. S. H. Song, W. K. Hong, S. S. Kwon and T. Lee, *Appl. Phys. Lett.*, 2008, **92**, 263109.
  26. M. Buscema, J. O. Island, D. J. Groenendijk, I. B. Sofya, G. A. Steele, S. J. V. Zant and A. C. Gmoez, *Chem. Soc. Rev.*, 2015, **44**.
  27. Q. L. Huang, F. D. Wang, P. D. Carpenter, D. Zemlyanov, D. Zakharov, E. A. Stach, W. E. Buhro and D. B. Janes, *Nano Lett.*, 2008, **8**, 49-55.
  28. C. Biswas, F. Güne, D. L. Duong, S. C. Lim, M. S. Jeong, D. Pribat and Y. H. Lee, *Nano Lett.*, 2011, **11**, 4682-4687.
  29. J. L. Zhu, G. W. Zhang, J. Q. Wei and J. L. Sun, *Appl. Phys. Lett.*, 2012, **101**, 123117-123117-4.
  30. Y. M. Shi, W. J. Fang, K. K. Zhang, W. J. Zhang and L. J. Li, *Small*, 2009, **5**, 2005-2011.



Negative photoconductivity is observed in InAs nanowires without surface defected layer, and is induced by gas adsorption and photogating effect.